

Implementation of a Madgwick Filter for Attitude Estimation

Vishnu Sashank Dorbala
UID 116907569

University of Maryland, College Park

Surabhi Verma
UID 116949460

University of Maryland, College Park

Late days used: 2

I. PROBLEM STATEMENT

Given the raw data from an Inertial Measurement Unit (IMU), our aim is to estimate its attitude using a Madgwick Filter. The IMU data contains angular velocities from a Gyroscope and accelerations from an Accelerometer, which are cleverly fused to obtain a Madgwick Filter outcome. Our results are compared with a ground truth attitude obtained from a VICON motion capture system. This system tracks a set of markers attached on the IMU rig, this giving us true estimate of the position and orientation of the object entirely from visual tracking. This approach is then evaluated on 10 different IMU datasets by analysing Euler angle plots from each of these sets.

II. DATA PRE-PROCESSING

We are given 6 Degree of Freedom (DoF) data from an Inertial Measurement Unit (IMU) in the order $[a_x \ a_y \ a_z \ \omega_x \ \omega_y]^T$. This corresponds to the linear acceleration along the x, y, z axis and the angular velocity about the z, x, y axis respectively. These readings, however, are not in their corresponding physical units. Given below is the conversion of a raw acceleration value along a given axis 'n' (a_n) into ms^{-2} .

$$\tilde{a}_n = (a_n * s_{a,n}) + b_{a,n}; n = x, y, z \quad (1)$$

Here, $b_{a,n}$ and $s_{a,n}$ represent the bias and scaling factors for acceleration along the n^{th} axis. These values are provided to us. For the raw angular velocity value (ω_n) about the n^{th} axis the conversion into physical units can be written in $rad s^{-1}$ as

$$\tilde{\omega}_n = \frac{3300}{1023} \times \frac{\pi}{180} \times 0.3 \times (\omega_n - b_{g,n}); n = x, y, z \quad (2)$$

where, $b_{g,n}$ is the gyroscope bias for the angular velocities about the n^{th} axis. The bias is calculated by taking the average of the first 200 values individually of each angular velocity. We also convert the VICON data, given in terms of rotation matrices in the Z-Y-X convention, into Euler angles. This is described as follows.

$$\begin{bmatrix} \phi \\ \theta \\ \psi \end{bmatrix} = \begin{bmatrix} atan2(r_{32}, r_{33}) \\ atan2(-r_{31}, \sqrt{r_{32}^2 + r_{33}^2}) \\ atan2(r_{21} + r_{11}) \end{bmatrix} \quad (3)$$

III. ATTITUDE ESTIMATION

In this section, we analyse 3 ways to estimate attitude from the given data.

A. Using Gyroscope Data

Given an estimate of the orientation $\hat{\mathbf{q}}_{E,t-dt}^S$ and angular velocity \mathbf{w}_{t-dt}^S at a prior timestamp $t - dt$, we can estimate the orientation $\mathbf{q}_{E,t}^S$ at time t . The rate of change of orientation in the quaternion format is described as follows:

$$\dot{\mathbf{q}}_{E,t-dt}^S = 0.5(\hat{\mathbf{q}}_{E,t-dt}^S * \mathbf{w}_{t-dt}^S), \quad (3)$$

where, $\mathbf{w}^S = [0 \ w_x \ w_y \ w_z]^T$ is the angular velocity quaternion in the sensor(S) frame. $\hat{\mathbf{q}}_{E,t-dt}^S$ is the prior estimate of the orientation of the earth(E) frame relative to the sensor(S) frame. For $t = 0$, $\hat{\mathbf{q}}_{E,t=0}^S = [1 \ 0 \ 0 \ 0]^T$ corresponding to 0 rotation about z axis. The solution of (3) is given as

$$\mathbf{q}_{E,t}^S = \hat{\mathbf{q}}_{E,t-dt}^S + \dot{\mathbf{q}}_{E,t-dt}^S dt \quad (4)$$

This orientation in the quaternion format $\mathbf{q}_{E,t}^S = [q0 \ q1 \ q2 \ q3]$ is converted into Euler angles $[\phi \ \theta \ \psi]$ as shown below.

$$\begin{bmatrix} \phi \\ \theta \\ \psi \end{bmatrix} = \begin{bmatrix} \arctan \frac{2(q_0 q_1 + q_2 q_3)}{1 - 2(q_1^2 + q_2^2)} \\ \arcsin(2(q_0 q_2 - q_3 q_1)) \\ \arctan \frac{2(q_0 q_3 + q_1 q_2)}{1 - 2(q_2^2 + q_3^2)} \end{bmatrix} \quad (5)$$

B. Using Accelerometer data

In the context of orientation filter, it is assumed that the accelerometer will measure only the gravitation vector $\hat{\mathbf{g}}^E = [0 \ 0 \ 0 \ 1]$. This measurement, described as $\hat{\mathbf{a}}^S = [0 \ a_x \ a_y \ a_z]$, is the gravity vector component in each of the x, y, and z axis of the sensor frame. Given $\hat{\mathbf{g}}$ relative to the E and S frame, we can optimize for the rotation quaternion. We use gradient descent in order to solve this optimization problem. Given an initial estimate of the orientation, $\hat{\mathbf{q}}_{E,t-dt}^S = [q1 \ q2 \ q3 \ q4]$ we can write the gradient descent equation as follows. Here, β is a variable that we finetune to 0.005 upon which, the attitude obtained appeared to follow the VICON data plot.

$$\hat{\mathbf{q}}_{E,t}^S = \hat{\mathbf{q}}_{E,t-dt}^S - \beta * \frac{\nabla f(\hat{\mathbf{q}}_{E,t-dt}^S, \hat{\mathbf{g}}^E, \hat{\mathbf{a}}_{t-dt}^S)}{\|\nabla f(\hat{\mathbf{q}}_{E,t-dt}^S, \hat{\mathbf{g}}^E, \hat{\mathbf{a}}_{t-dt}^S)\|}$$

$$\begin{aligned}
& \nabla f(\hat{\mathbf{q}}_{E,t-dt}^S, \hat{\mathbf{g}}^E, \hat{\mathbf{a}}_{t-dt}^S) = \\
& J^T(\hat{\mathbf{q}}_{E,t-dt}^E, \hat{\mathbf{g}}^E) f(\hat{\mathbf{q}}_{E,t-dt}^S, \hat{\mathbf{g}}^E, \hat{\mathbf{a}}_{t-dt}^S) \\
& J(\hat{\mathbf{q}}_{S,t-dt}^E, \hat{\mathbf{g}}^E) = \begin{bmatrix} -2q_3 & 2q_4 & -2q_1 & 2q_2 \\ 2q_2 & 2q_1 & 2q_4 & 2q_3 \\ 0 & -4q_2 & -4q_3 & 0 \end{bmatrix} \\
& f(\hat{\mathbf{q}}_{E,t-dt}^S, \hat{\mathbf{g}}^E, \hat{\mathbf{a}}_{t-dt}^S) = \begin{bmatrix} 2(q_2q_4 - q_1q_3) - a_x \\ 2(q_1q_2 + q_3q_4) - a_y \\ 2(\frac{1}{2} - q_2^2 - q_3^2) - a_z \end{bmatrix} \quad (5)
\end{aligned}$$

C. Using a Madgwick Filter

A Madgwick filter simply put, is a better version of complementary filter. This is because we perform all computations in a quaternion space, which for certain operations (such as matrix multiplication), is a lot more computationally effective than it's Euler counterparts. This makes it a practically viable for usage in several robotic applications. Dealing with quaternions also allows one to obtain unique rotations.

The outcome of the Madgwick filter is obtained by fusing the accelerometer and the gyroscope data readings as shown below. For this case, β is set to 0.01.

$$\begin{aligned}
\dot{\mathbf{q}}_{S,t-dt}^E &= \dot{\mathbf{q}}_{E,t-dt}^S - \beta \frac{\nabla f(\hat{\mathbf{q}}_{E,t-dt}^S, \hat{\mathbf{g}}^E, \hat{\mathbf{a}}_{t-dt}^S)}{\|\nabla f(\hat{\mathbf{q}}_{E,t-dt}^S, \hat{\mathbf{g}}^E, \hat{\mathbf{a}}_{t-dt}^S)\|} \\
\mathbf{q}_{S,t+1}^E &= \mathbf{q}_{S,t-dt+1}^E + \dot{\mathbf{q}}_{S,t-dt}^E dt \quad (6)
\end{aligned}$$

IV. PLOTS AND ANALYSIS

In this section, we show the orientation plots obtained in our experiments. There are 30 different plots from 10 sets of raw data. For the first 6 set of plots (the training set), we also plot the VICON data. For the remaining 4 plot sets (the test set), no VICON values are not available.

Each set(page) contains 3 plots showing attitude estimates in the order ψ , θ and ϕ corresponding to rotation about z axis, the new y axis and the new x axis. Each plot inturn contains at least 3 graphs, corresponding to the Gyroscope, the accelerometer, and the Madgwick Filter outcomes. For the first 6 sets of raw data, we include the ground truth VICON data plots. All rotations are plotted in radians. Furthermore, absolute value of the time stamp is not considered. Instead, time is assumed to start from $t = 0$.

In most of the plots, the Madgwick Filter appears to follow the curve of the VICON data. It seems to be an average of the accelerometer and gyroscope outcomes. This is true for the ϕ , θ and ψ plots for the sequences 1-5.

In plot 6, there are some gaps in the VICON plot where there is no data. A plausible reason for this might be that a reset signal might have been fired on the VICON, due to which no data was captured during that time. It could also be a case of hidden VICON markers during motion, due to which no attitude could be estimated at that particular instance.

On the test data sets 7-10, the ground truth VICON data is unavailable. For our case in these sets, we observe that the

Madgwick Filter plot seems to follow the Gyroscope outcome more closely than the accelerometer output. This might be due to the fact that we obtain gyroscope orientation by directly integrating the angular velocity, which is far less sophisticated than the computation of orientation angles from accelerometer data.

V. ROTPLOT VIDEOS

In order to understand the outcomes in 3D, we create an object that orients itself according to the outputs of the accelerometer, gyroscope and the Madgwick filter. These 'rot-plot' outcomes have been uploaded here.¹

VI. LESSONS LEARNT

An important lesson we learnt was the importance of calibrating the bias of the gyroscope accurately before performing any future computations. During implementation, we observed that using wrong bias values to initialize the gyroscope data (even by small amounts) lead to drastically different outcomes. Although this seemed counter intuitive at first, it made sense later when we observed of how effective scaling improved our results.

VII. CONCLUSION

In conclusion, we observe that using the Madgwick Filter to compute orientation performs a lot better than using only an accelerometer or a gyroscope. This could be attributed to the fact that the Madgwick filter fuses data from the accelerometer and the gyroscope, to achieve a best of both worlds scenario. We also observe that the performance of the Complementary Filter is very similar, but because the Madgwick filter relies on using quaternion transforms, it is a lot less computationally intensive. This is especially favourable for robotic applications such as drones that require energy to be used judiciously.

VIII. ACKNOWLEDGMENTS

We would like to thank the Teaching Assistants of the course, Abhinav Modi and Prateek Arora, as well as the instructors, Nitin. J. Sanket and Chahat Deep Singh for their advice and constant guidance throughout the course of this assignment.

IX. REFERENCES

- Madgwick Filter Tutorial - [Link](#)
- Madgwick Filter Paper - [Link](#)
- Pyquaternion Library - [Link](#)
- Working with Quaternions - [Link](#)
- Visualizing Quaternions - [Link](#)

¹Link to Rotplots

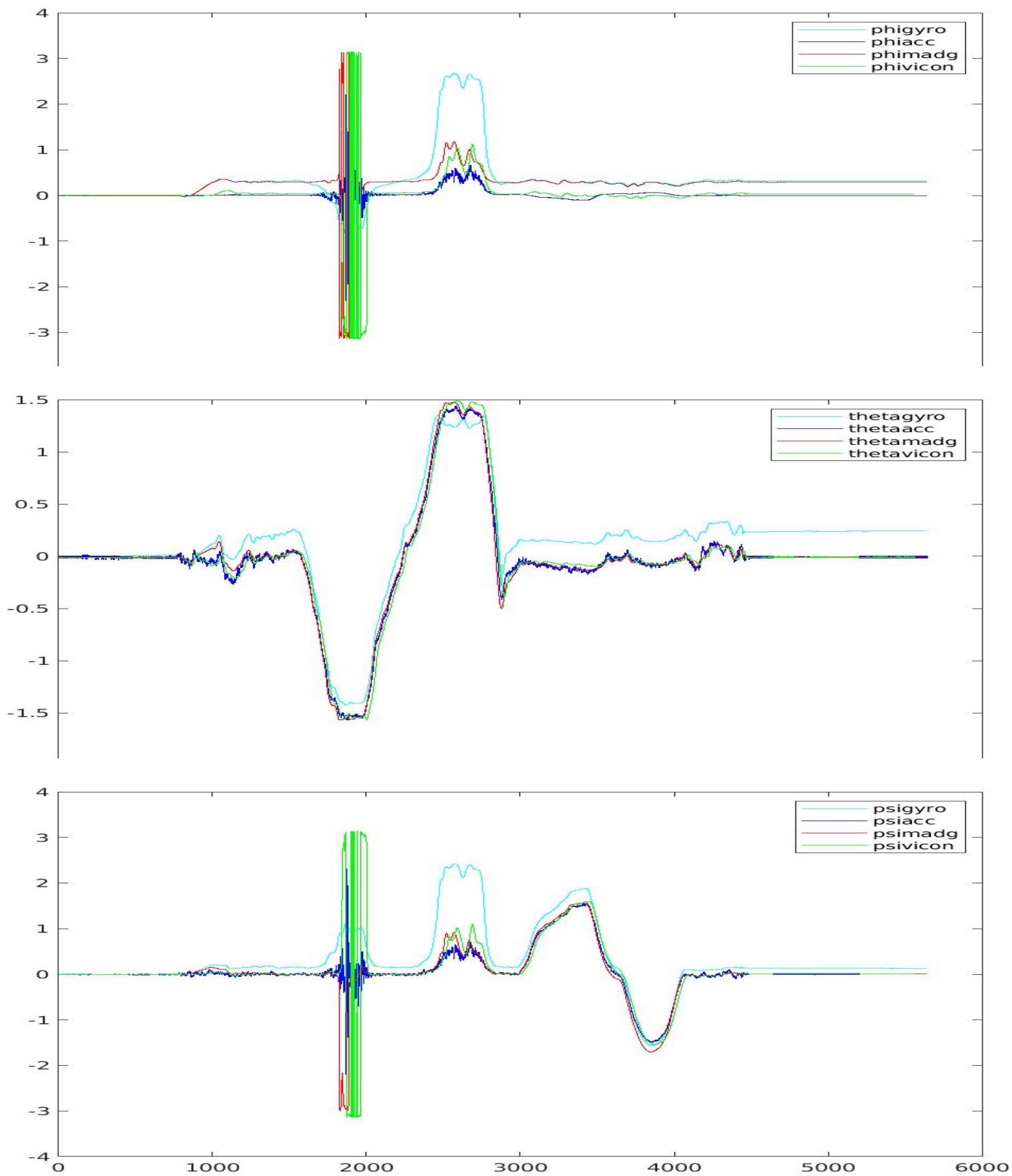


Fig. 1: Raw 1

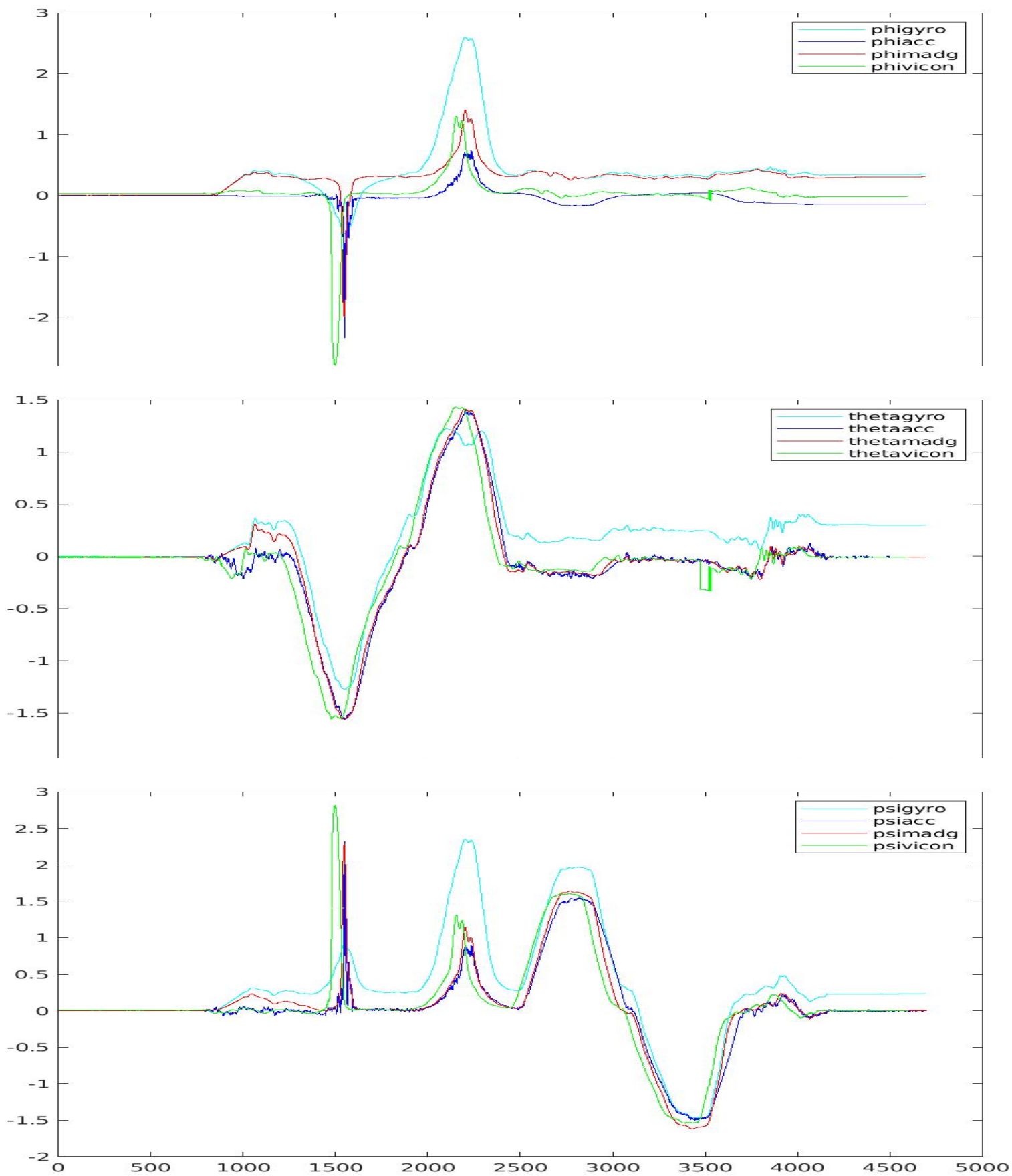


Fig. 2: Raw 2

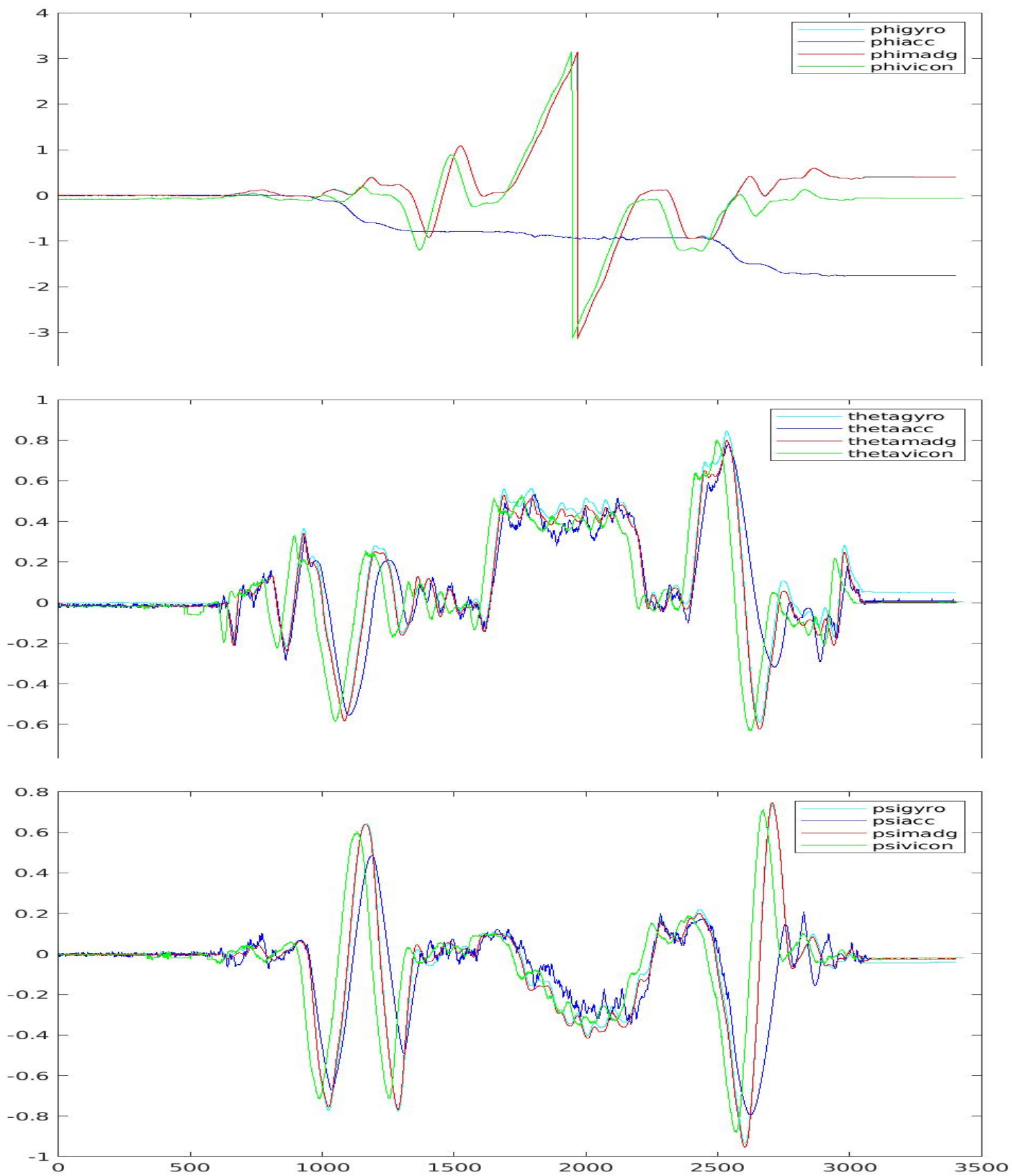


Fig. 3: Raw 3

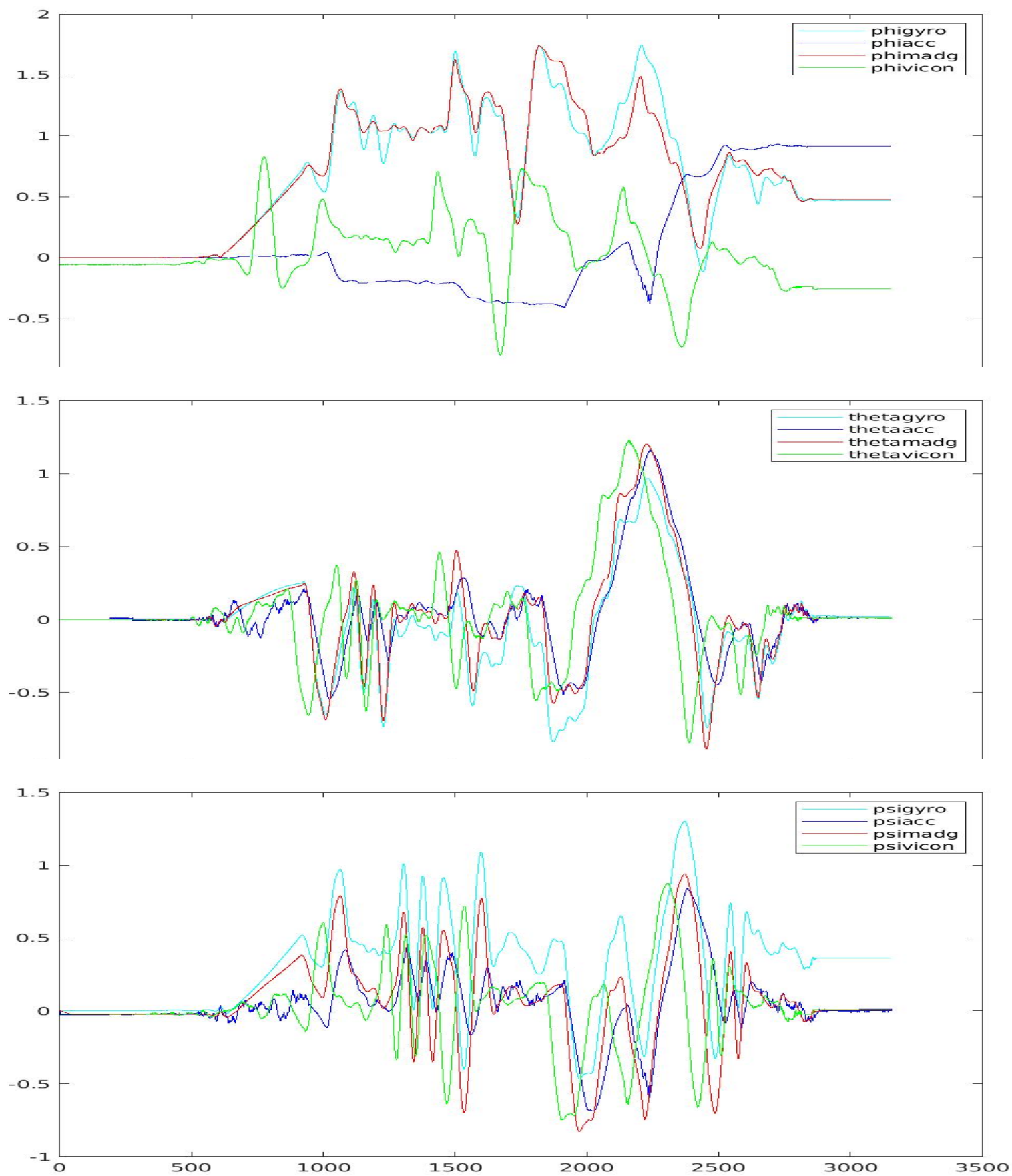


Fig. 4: Raw 4

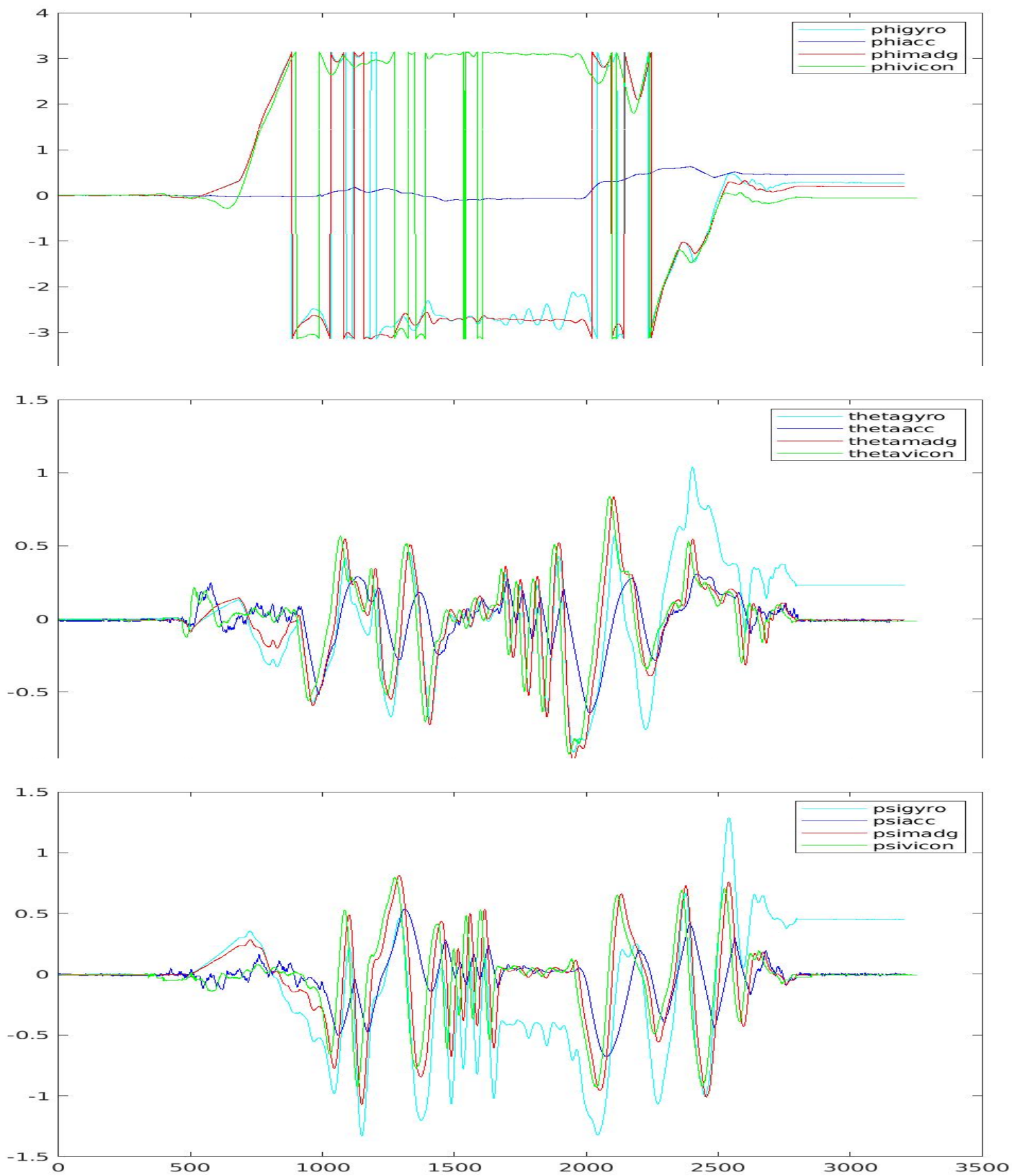


Fig. 5: Raw 5

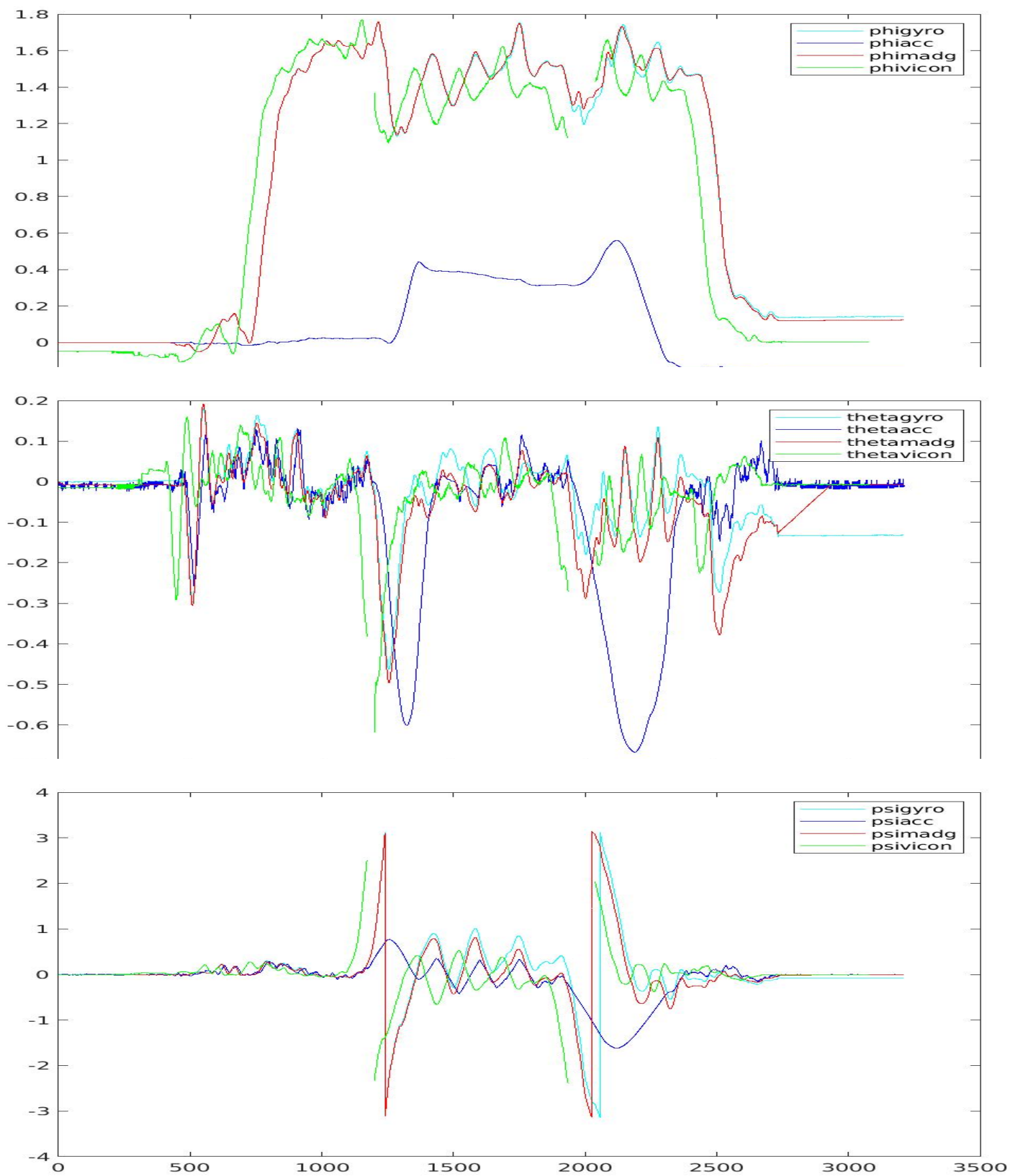


Fig. 6: Raw 6

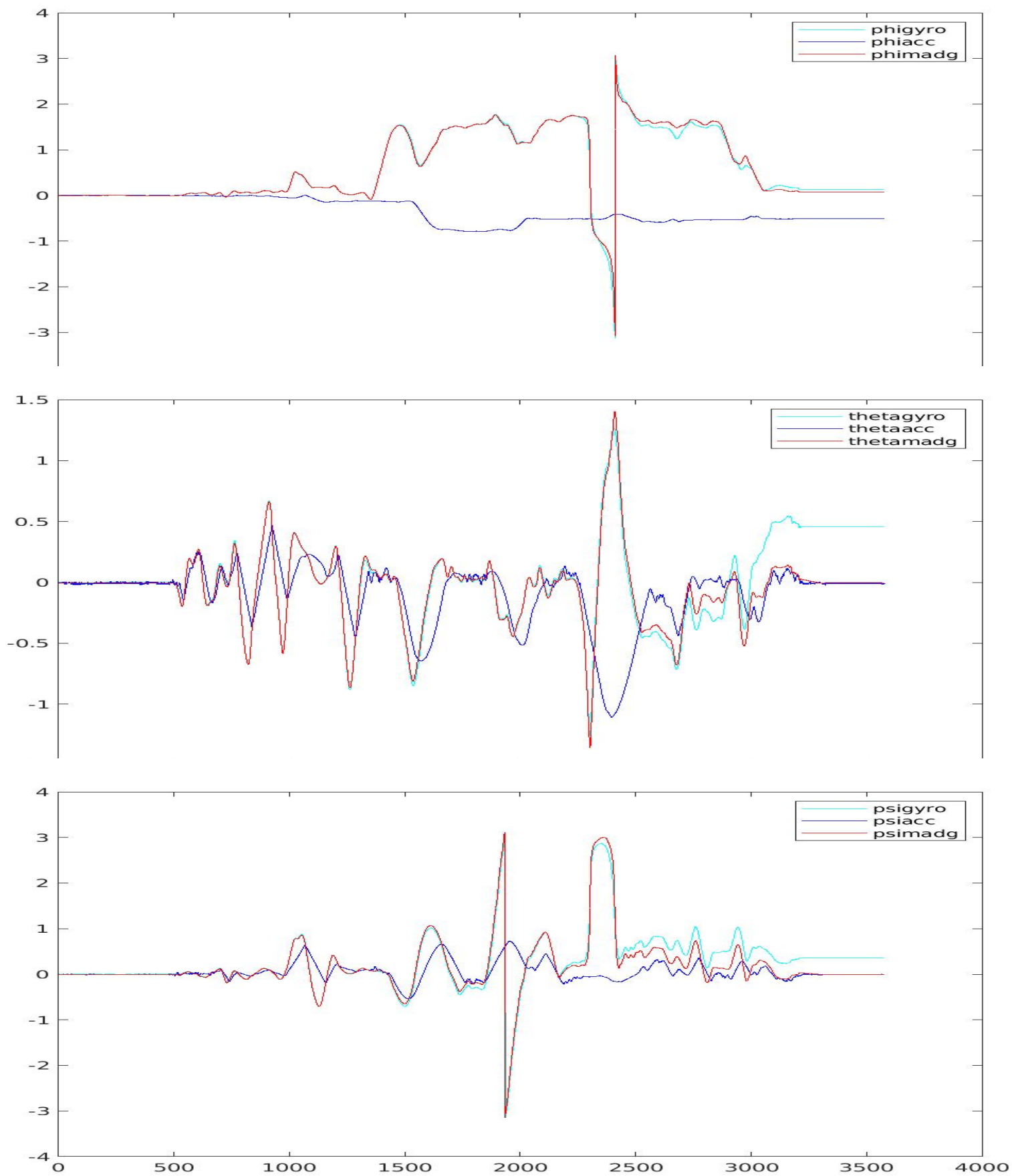


Fig. 7: Raw 7

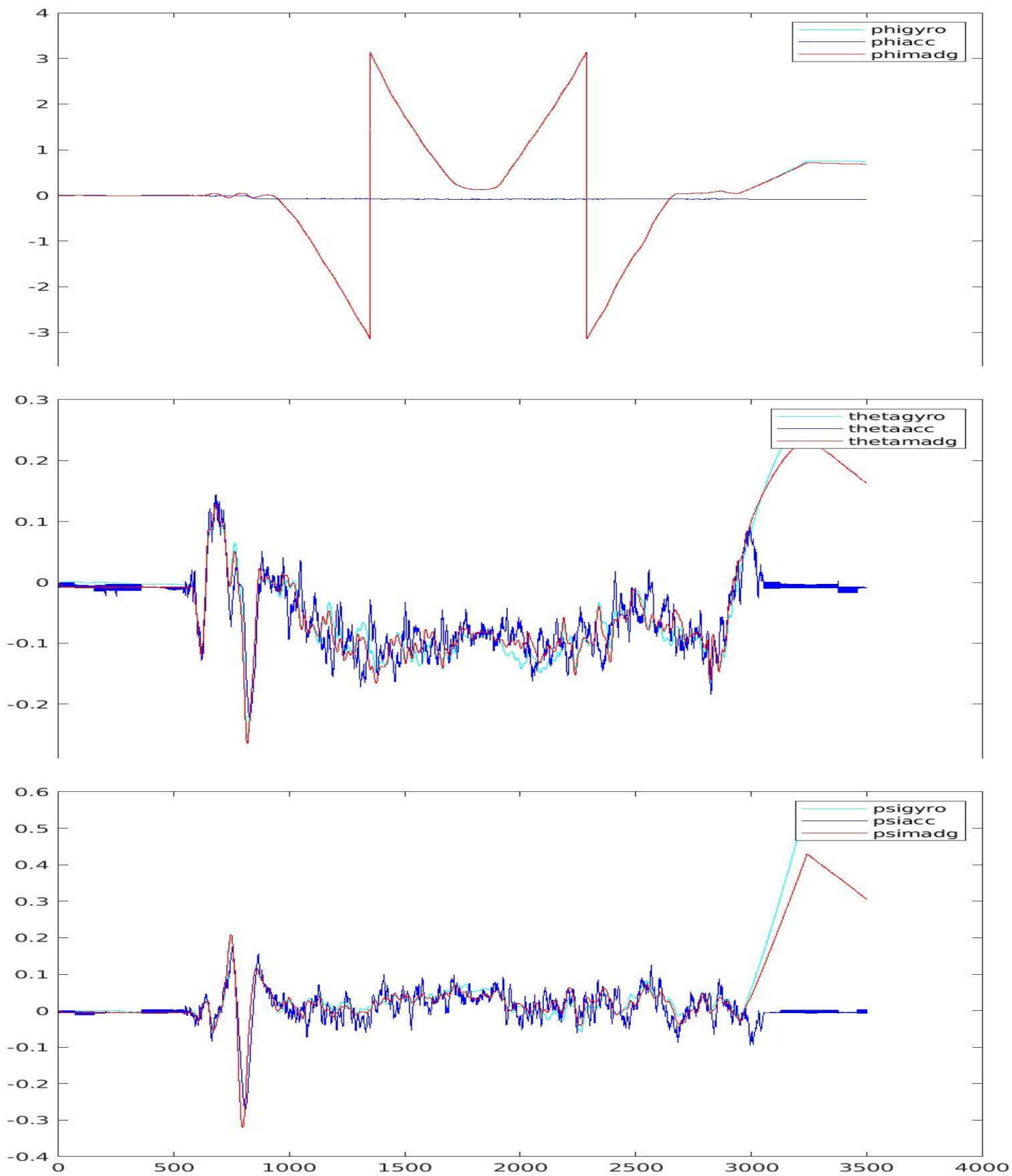


Fig. 8: Raw 8

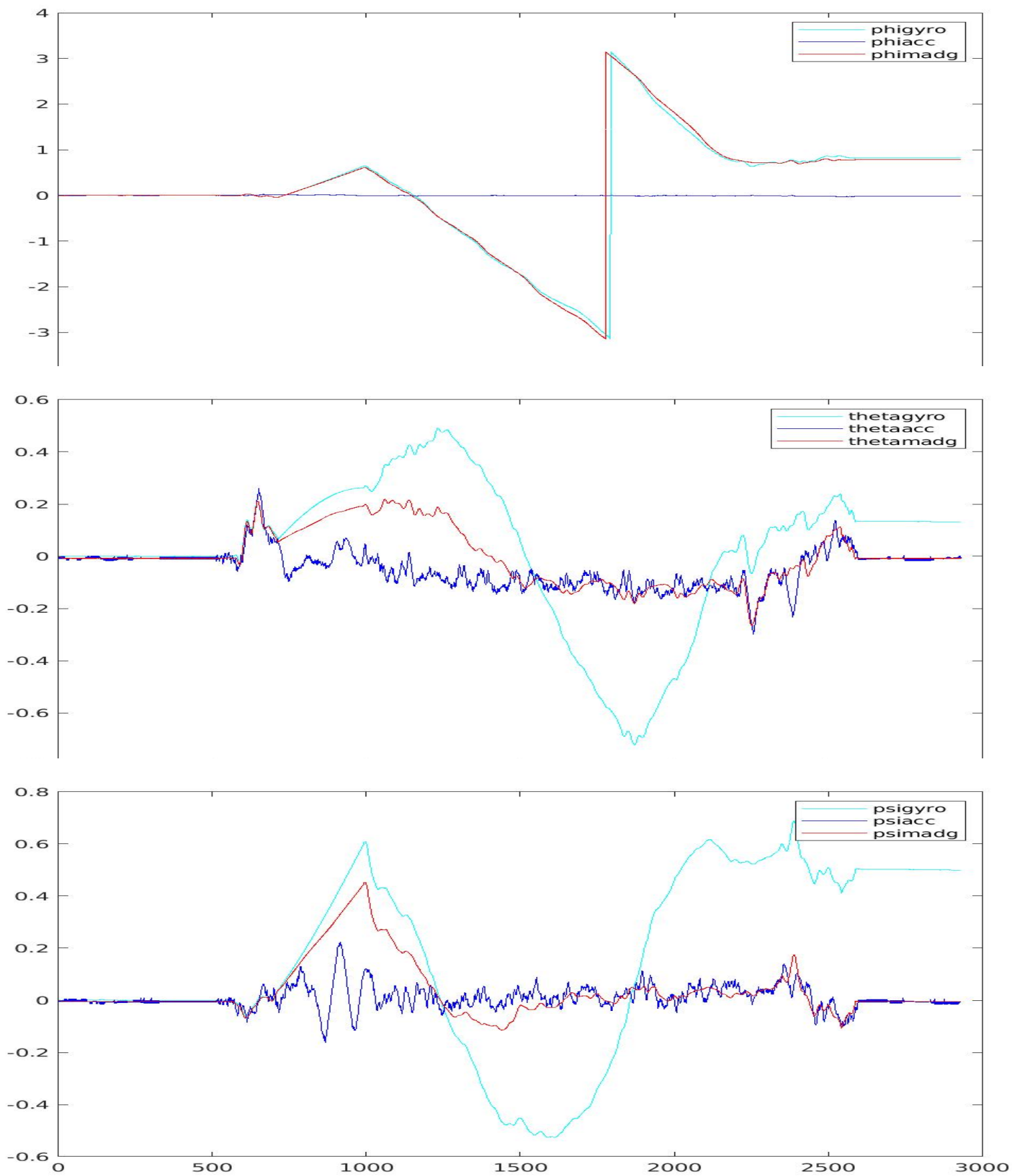


Fig. 9: Raw 9

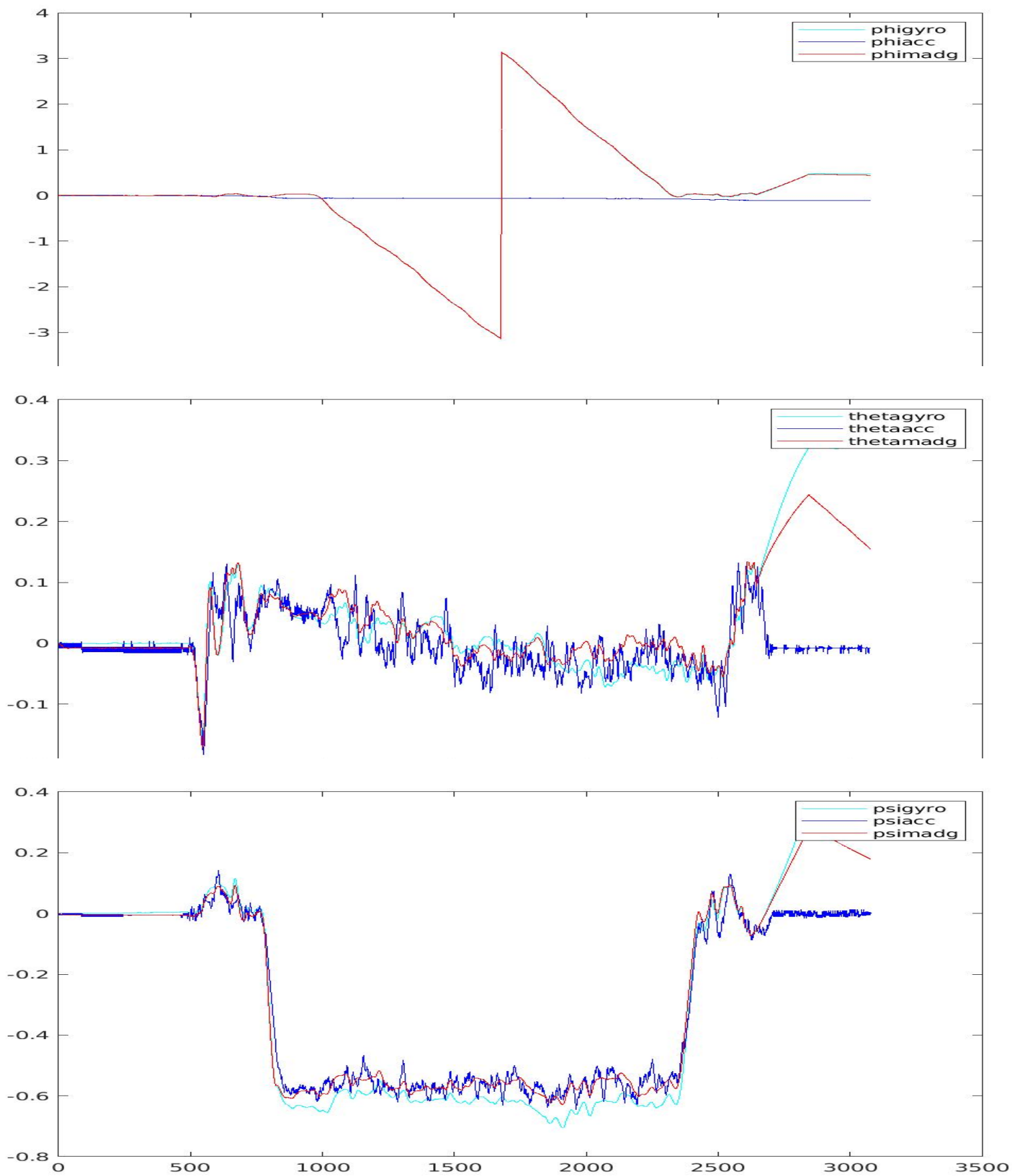


Fig. 10: Raw 10